Appeared in Proc. of Artificial Neural Networks in Engineering (ANNIE), (St. Louis, USA), November 2006

A NEW BIOMETRIC MODALITY BASED ON CONJUNCTIVAL VASCULATURE

REZA DERAKHSHANI
Dept. of CS and Electrical Eng.
School of Computing and Eng.
University of Missouri Kansas City
Kansas City, Missouri
derakhshanir@umkc.edu

ARUN ROSS
Lane Department of Computer
Science and Electrical Engineering,
West Virginia University,
West Virginia
arun.ross@mail.wvu.edu

SIMONA CRIHALMEANU
Lane Department of Computer
Science and Electrical Engineering,
West Virginia University, West Virginia
simona.crihalmeanu@mail.wvu.edu

ABSTRACT
A new biometric indicator based on the patterns of conjunctival vasculature is proposed. Conjunctival vessels can be observed on the visible part of the sclera that is exposed to the outside world. These vessels demonstrate rich and specific details in visible light, and can be easily photographed using a regular digital camera. In this paper we discuss methods for conjunctival imaging, preprocessing, and feature extraction in order to derive a suitable conjunctival vascular template for biometric authentication. Commensurate classification methods along with the observed accuracy are discussed. Experimental results suggest the potential of using conjunctival vasculature as a biometric measure.

INTRODUCTION

Biometrics is the science of estbalishing the identity of individuals based on their unique physical or behavioral traits (Jain et al. 1999). Compared to other traditional authentication methods such as ID cards and passwords, the use of biometric traits is considered to be more convenient and secure as an individual's biological traits cannot be lost, forgotten or easily stolen. Among all biometric traits, eye-based methods in general and iris recognition in particular have been considered to be more accurate and reliable (Daugman 1993, Wildes 1997). However, the performance of an iris recognition system is affected by the quality of the acquired images. In particular, the presentation of non-frontal iris images to a biometric system, e.g., due to off-axis gaze directions with respect to the imaging device, can result in inferior matching performance.

Besides the iris, human eyes carry other specific and identifiable patterns. One such pattern arises from the vasculature seen on the sclera, the white part of the eye ball. Most notably, when the camera acquires a non-frontal image of the iris, vascular information of the sclera is revealed. In this paper, we introduce and discuss a new modality for eye-borne personal identification using the patterns of ocular surface vessels residing in the episclera and conjunctiva. Incorporation of this modality in an iris system is also expected to decrease the threat of spoof attacks since it can be difficult to accurately replicate these vessels using physical artifacts.

Appeared in Proc. of Artificial Neural Networks in Engineering (ANNIE), (St. Louis, USA), November 2006

OCULAR SURFACE VASCULATURE

Human recognition using vascular patterns in the human body has been studied in the context of fingers (Miura et al. 2004), palm (Lin and Fan 2004) and retina (Hill 1999). In the case of retinal biometrics, an especial optical device for imaging the back of the eyeball is needed (Hill 1999). Due to its perceived invasiveness and the required degree of subject cooperation, the use of retinal biometrics may not be acceptable to some individuals.

The conjunctiva is a thin, transparent, and moist tissue that covers the outer surface of the eye. The part of the conjunctiva that covers the inner lining of the eyelids is called palpebral conjunctiva, and the part that covers the outer surface of the eye is called ocular (or the bulbar) conjunctiva, which is the focus of this study. The ocular conjunctiva is very thin and clear; thus the vasculature (including those of the episclera) is easily visible through it. The visible microcirculation of conjunctiva offers a rich and complex network of veins and fine microcirculation (Fig. 1). The apparent complexity and specificity of these vascular patterns motivated us to utilize them for personal identification (Derakhshani and Ross 2006).

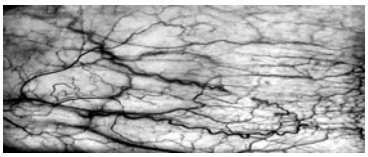

Fig. 1 Enhanced image of ocular vasculature as seen on the sclera.

We have found conjunctival vasculature to be a suitable biometric as it conforms to the following criteria (Jain et al. 2004):

Universality: All normal living tissues, including that of the conjunctiva and episclera, have vascular structure.

Uniqueness: Vasculature is created during embryonic vasculogenesis. Its detailed final structure is mostly stochastic and, thus, unique. Even though no comprehensive study on the uniqueness of vascular structures has been conducted, study of some targeted areas such as those of the eye fundus confirm the uniqueness of such vascular patterns, even between identical twins (Simon and Goldstein 1935, Tower 1955).

Permanence: Other than cases of significant trauma, pathology, or chemical intervention, spontaneous adult ocular vasculogenesis and angiogenesis does not easily occur. Thus, the conjunctival vascular structure is expected to have reasonable permanence (Joussen 2001).

Practicality: Conjunctival vasculature can be captured with commercial off the shelf digital cameras under normal lighting conditions, making this modality highly practical.

Acceptability: Since the subject is not required to stare directly into the camera lens, and given the possibility of capturing the conjunctival vasculature from several feet away, this modality is non-intrusive and thus more acceptable.

Spoof-proofness: The fine, multi surface structure of the ocular veins makes them hard to reproduce as a physical artifact.

Besides being a stand-alone biometric modality, we anticipate that the addition of conjunctival biometrics will enhance the performance of current iris-based biometric system in the following ways:

(a) Improving accuracy by the addition of vascular features.

(b) Facilitating recognition using off-angle iris images. For instance, if the iris information is relegated to the left or right portions of the eye, the scleral

Appeared in Proc. of Artificial Neural Networks in Engineering (ANNIE), (St. Louis, USA), November 2006

vein patterns will be further exposed. This feature makes scleral vasculature a natural complement to the iris biometric.

(c) Addressing the failure-to-enroll issue when iris patterns are not usable (e.g., due to surgical procedures)

(d) Reducing vulnerability to spoof attacks. For instance, when implemented alongside iris systems, an attacker needs to reproduce not only the iris but also different surfaces of the sclera along with the associated microcirculation, and make them available on commensurate eye surfaces.

IMAGE ACQUISITION AND PROCESSING

Image Capture

The vascular patterns of the sclera can be imaged while the subject is (a) looking straight into the camera, (b) to the left, (c) to the right, (d) or up; yielding a total of four different capturing poses. These images, individually or collectively, can be used for conjunctival vascular identification. When fusing conjunctival information with iris scans for multimodal eye biometrics, the conjunctiva and the iris may be imaged and segmented simultaneously, making this a convenient acquisition methodology.

For this study, we obtained a close up RGB image of 12 eyes (left and right eyes, six subjects) using a commercial 5 MP Sony® digital camera. A second picture was taken in the same manner for matching purposes. Segmentation of the region of interest - a rectangular scleral area beneath the iris - was performed manually for this initial study. The goal of this study is to demonstrate the feasibility of using the vascular structure of the sclera for biometric identification. We used the MATLAB®7 software running on a Pentium® IV based personal computer for performing the following operations.

Image Preprocessing

Enhancement: The purpose of image enhancement is to facilitate the isolation of vasculature from scleral background. Image enhancement was accomplished in two steps. First, a contrast-limited adaptive histogram equalization (CLAHE) scheme was applied to the region of interest in order to enhance the color image. We used the green layer of the RGB image as it leads to a better contrast between the blood vessels and the background (Owen et al. 2002). A selective line enhancement scheme, as described in (Li et al. 2003), was used to enhance the blood vessels of the green channel. This process effectively locates lines and curves whilst suppressing objects of other shapes. The algorithm is based on the second derivatives, using the Hessian matrix $H = \begin{bmatrix} I_{xx} & I_{xy} \\ I_{yx} & I_{yy} \end{bmatrix}$, of the intensity image. However, since derivatives are sensitive to noise, the image is first convolved with a Gaussian function whose standard deviation, σ, represents the scale of the lines and implicitly, the girth of the blood vessels being detected. For every pixel in the image, two eigenvalues of the Hessian matrix are computed:

$$\lambda_1 = K + \sqrt{K^2 - Q^2}, \quad \lambda_2 = K - \sqrt{K^2 - Q^2}$$

where $K = \frac{I_{xx} + I_{yy}}{2}, Q = \sqrt{(I_{xx} I_{yy} - I_{xy} I_{yx})}$

Each pixel of the enhanced image is obtained as

$$I_{line}(\lambda_1, \lambda_2) = \begin{cases} |\lambda_1| - |\lambda_2|, & if\ \lambda_1 < 0 \\ 0, & if\ \lambda_1 \geq 0 \end{cases}$$

Appeared in Proc. of Artificial Neural Networks in Engineering (ANNIE), (St. Louis, USA), November 2006

Since the veins are of different thickness over the image, a multiscale, iterative Gaussian enhancement filter with varying σ is needed. This iterative procedure is summarized below.

1- Empirically determine the range of vessel calibers and define (σ_1, σ_2,… σ_N) accordingly.

2- For i=1, 2,… N:

a. Smooth the original image with a 2D Gaussian with parameter σ_i;

b. For each pixel in the smoothed image, compute the Hessian matrix and its two eigenvalues;

c. For each pixel compute the line-enhanced image, I_{line};

d. Multiply the output by σ_i^2 to normalize intensity.

3-The final value of a pixel in the enhanced image is obtained as the maximum of the outputs corresponding to all the σ_i's. A sample image using the above enhancement operation is shown in Fig. 2.

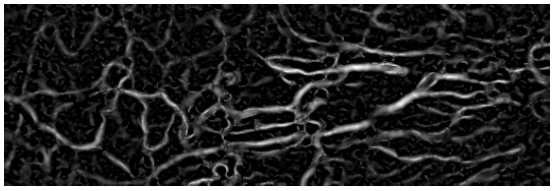

Fig. 2 Filtered image using the multiscale iterative algorithm.

Tracing scleral veins: Given the fine structure of blood vessels, edge-detection based segmentation techniques do not provide acceptable results. Therefore, we used a "region growing" method to obtain a binarized representation of conjunctival vascular trees (Perez 1999). The mentioned region growing method is an iterative labeling algorithm that classifies a pixel as foreground (i.e., blood vessel, V) or background (B). The algorithm first binarizes the image using Otsu's threshold to provide an initial categorization of the pixels into the two classes, V and B. It then uses the information provided by the local intensity values and image gradient magnitudes to determine the final labels. The algorithm proceeds as follows:

1-A set of seed pixel locations for V and B classes, satisfying $I_{line} \geq \mu_V$ for V and $I_{line} \leq \mu_B$ for B, are identified. σ_V, σ_B, μ_V, and μ_B are the standard deviations and means of the background and vessel pixels, respectively.

2- Each V seed expands into its neighbors if

$$\begin{cases} (\mu_V - a_V \sigma_V) \leq I_{line} \\ |\nabla(I_{line})| \leq (\mu_G + a_G \sigma_G) \\ N_V \geq 1 \end{cases}$$

Similarly, a B seed expands into its neighbors if

$$\begin{cases} I_{line} \leq (\mu_B + a_B \sigma_B) \\ |\nabla(I_{line})| \leq \mu_G \\ N_B \geq 1 \end{cases}$$

a_V and a_B are user-defined parameters, and N_V and N_B are the number of neighboring pixels satisfying the above conditions. This step is iterated over while incrementing the parameters a_V and a_B by 0.5 between iterations.

3- The vessel and background pixels are allowed to grow simultaneously once again but this time without any gradient restrictions:

Appeared in Proc. of Artificial Neural Networks in Engineering (ANNIE), (St. Louis, USA), November 2006

$$\begin{cases} (\mu_V - a_V\sigma_V) \le I_{line} \le (\mu_V + a_V\sigma_V) \\ N_V \ge 1 \end{cases}$$
$$\begin{cases} (\mu_B - a_B\sigma_B) \le I_{line} \le (\mu_B + a_B\sigma_B) \\ N_B \ge 1 \end{cases}$$

The result of this region growing algorithm is a binary image of the underlying vasculature as shown in Fig. 3.

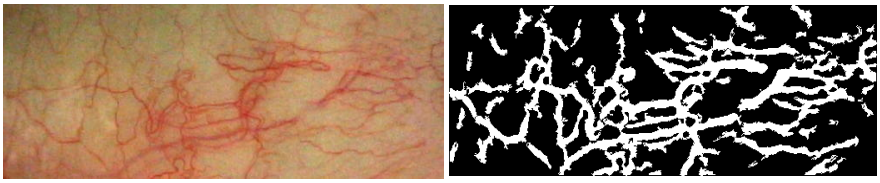

Fig. 3: The result of region growing algorithm on conjunctival vasculature. Top: unprocessed image, bottom: processed image.

Classification

For the verification or identification phase, the claimant's template is matched against his or her stored template for verification (one-to-one matching), or against the whole database of templates in the case of identification (one-to-many matching). Two different methods for coarse and fine level matching are explained below.

To reduce the search time for large databases, we propose a multi-level classification scheme. First, a coarse level procedure using a small template is used to rapidly find a subset containing the most probable matches. Then, a second but more complex algorithm, determines the best match from this subset.

1-Coarse-level matching:

For a fast, coarse-level identification of the target subset of images we utilized Hu's invariant moments as features (Hu 1962). These moments are invariant with respect to affine transforms (shifting, rotation, and scaling). The seven Hu moments are obtained as follows.

The (p+q) moment of a gray level digital image with intensity values *f(x,y)* is defined by:

$$M_{pq} = \sum_x \sum_y x^p y^q f(x,y)$$

From this we have:

$$\bar{x} = \frac{M_{10}}{M_{00}},\ \bar{y} = \frac{M_{01}}{M_{00}}$$

The central moments of the image are defined as,

$$\mu_{pq} = \sum_x \sum_y (x-\bar{x})^p (y-\bar{y})^q f(x,y)$$

The central moments used in Hu invariant moments are given by

$\mu_{00}=M_{00}$, $\mu_{01}=\mu_{10}=0$, $\mu_{11}=M_{11}-\bar{x}M_{01}$, $\mu_{20}=M_{20}-\bar{x}M_{10}$, $\mu_{02}=M_{02}-\bar{y}M_{01}$,
$\mu_{21}=M_{21}-\bar{x}M_{11}-\bar{y}M_{20}+2\bar{x}^2M_{01}$, $\mu_{12}=M_{12}-\bar{y}M_{11}-\bar{x}M_{02}+2\bar{y}^2M_{10}$,
$\mu_{30}=M_{30}-3\bar{x}M_{20}+2\bar{x}^2M_{10}$, and $\mu_{03}=M_{03}-3\bar{y}M_{02}+2\bar{y}^2M_{01}$.

Appeared in Proc. of Artificial Neural Networks in Engineering (ANNIE), (St. Louis, USA), November 2006

Hu's invariant moments I_j, j=1, 2,…, 7, are derived from the above moments in a fashion that makes them invariant under affine transforms:

$$I_1 = \mu_{20} + \mu_{02}$$
$$I_2 = (\mu_{20} - \mu_{02})^2 + 4\mu_{11}^2$$
$$I_3 = (\mu_{30} - 3\mu_{12})^2 + (3\mu_{21} - \mu_{03})^2$$
$$I_4 = (\mu_{30} + \mu_{12})^2 + (\mu_{21} + \mu_{03})^2$$
$$I_5 = (\mu_{30} - 3\mu_{12})(\mu_{30} + \mu_{12})\left((\mu_{30} + \mu_{12})^2 - 3(\mu_{21} + 3\mu_{03})^2\right) +$$
$$(3\mu_{21} - \mu_{03})(\mu_{21} + \mu_{03})\left(3(\mu_{30} + \mu_{12})^2 - (\mu_{21} + \mu_{03})^2\right)$$
$$I_6 = (\mu_{20} - \mu_{02})\left((\mu_{30} + \mu_{12})^2 - (\mu_{21} + \mu_{03})^2 + 4\eta_{11}(\mu_{30} + \mu_{12})(\mu_{21} + \mu_{03})\right)$$
$$I_7 = (3\mu_{21} - \mu_{03})(\mu_{30} + \mu_{12})\left((\mu_{30} + \mu_{12})^2 - 3(\mu_{21} + 3\mu_{03})^2\right)$$
$$+ (\mu_{30} - 3\mu_{12})(\mu_{21} + \mu_{03})\left(3(\mu_{30} + \mu_{12})^2 - (\mu_{21} + \mu_{03})^2\right)$$

During the course of the experiments with the 24-image dataset, we found that the skew-invariant seventh moment resulted in the best performance. This performance was evaluated by a Euclidian separation metric of the Hu features. In order to calculate this metric, we first chose a feature vector *h* whose elements are a subset of Hu invariant moments:

$$\overrightarrow{h_i^k} = [I_a\ I_b\ \ldots],$$

where k is the capture session (here k=1 for enrollment and k=2 for identification), i is the subject number, and a, b,…∈{1, 2,…7} indicate the selected Hu moments. One separation metric for the choice of Hu moments is given by,

$$r = \frac{tr(D)}{\sum_{i=1}^{N}\sum_{j=1,j\neq i}^{N} d_{ij}}$$

where $D_{N\times N} = [d_{ij}]$ is the pair-wise Euclidean distance matrix between two Hu features, i.e. $d_{ij} = \left\| \overrightarrow{h_i^1} - \overrightarrow{h_j^2} \right\|$, with i and j indicating the subject number out of an N-subject dataset with 2N scleral shots (N enrollment, N verification). Accordingly, a lower *r* indicates a better Hu feature set *h* as the same-subject inter-capture distance (numerator) will be smaller while the distance between non-matching subjects (denominator) will be larger.

Results: Using our dataset, the 7th Hu feature yielded a misidentification of 3.47% across all possible pair-wise matches, with an *r* value of 0.0105. We used the adaptive histogram-equalized output of the green layer of input RGB images for estimating the $\overrightarrow{h_i^k}$ feature vectors. Given these results, one can choose a subset of identities corresponding to the closest enrolled $\overrightarrow{h_i^k}$, and transmit only the top matches (three in our experiments) to the next phase for more detailed matching.

2-Detailed matching:

This second step acts upon the short list generated in the previous step. Since this step is based on minutiae matching, it needs a reliable skeleton binary image of the conjunctival vasculature. In order to find the centerlines of the detected blood vessels, the

Appeared in Proc. of Artificial Neural Networks in Engineering (ANNIE), (St. Louis, USA), November 2006

images were post-processed using the following morphological operations: (a) Isolated foreground pixels were removed. (b) The edges of the blood vessels were smoothed according to the following rule: a pixel is set to 1 if there are five or more pixels in its 3×3 neighborhoods; otherwise the pixel is set to 0. (c) Foreground curves were thinned to a width of one pixel which denotes the centerline of vessels. (d) Spur pixels were removed.

Minutiae selection: In order to represent the blood vessel patterns using discrete points, the locations of vascular branching (anastamosis points) were used to generate the template corresponding to each eye. These points are referred to as minutiae points. Fig. 4 shows the different detected minutiae points in an image. Using our small pilot dataset, the identification (one to many matching) result of our minutiae point matching algorithm was 100%, It must be noted that as the size of the dataset increases, the error rate is bound to increase. One of the goals of this research in general is to understand the uniqueness and permanence of these minutiae points.

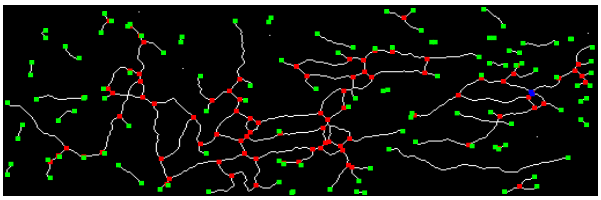

Figure 4: Minutiae detected on the skeleton image.

Given successful segmentation, a simple 2D correlation of the negative of the preprocessed image can also be used for identification, with the highest correlation indicating a match. Using the negative of the adaptive-histogram equalized green layer images, we obtained 100% identification using this computationally intensive but simple scheme. We are in the process of collecting a larger database in order to establish the uniqueness and permanence of this biometric trait.

CONCLUSIONS AND FUTURE WORK

We have introduced a new, convenient modality based on conjunctival vasculature for eye-based biometrics. These patterns exist in the visible light as well as near-infrared images of the eye. Besides their potential as a standalone biometric authentication, scleral vascular scans have the immediate benefit of adding precision and security to existing iris biometric systems. Initial results look promising and underscore the necessity for pursuing further research in this area.

For future work, we intend to do a long term analysis on a larger population to further study time-invariance, uniqueness, and universality of the scleral vasculature patterns. We will also study the scalability of our two-tier classification system, as well as the possibility of incorporating conjunctival information with iris scan systems. Finally, we will evaluate the spoof-protection capabilities of the proposed biometric under different scenarios.

AKNOWLEDGMENTGS

The authors wish to thank Dr. Rohit Krishna (UMKC Medical School) for his invaluable suggestions and contributions. We are also grateful for the assistance of our

Appeared in Proc. of Artificial Neural Networks in Engineering (ANNIE), (St. Louis, USA), November 2006

graduate students Ashish Anand and Chen Cheng (CSEE, UMKC), and Chris Boyce (CSEE, WVU) for their help in acquiring and processing the images. The Hu moments were calculated using programs developed by Vivek Kwatra at Georgia Tech (http://www-static.cc.gatech.edu/~kwatra/). This work was supported in part by a grant from Center for Identification Technology Research (CITeR), an NSF IUCRC center at West Virginia University, Morgantown, WV.

REFERENCES

A. K. Jain, R. Bolle, and S. Pankanti (Eds) 1999, "*BIOMETRICS: Personal Identification in Networked Society*," Kluwer Academic Publishers.

J. G. Daugman, 1993 "High confidence visual recognition of persons by a test of statistical independence," *IEEE Transactions on Pattern Analysis and Machine Intelligence*, vol. 15, no. 11, pp. 1148–1160.

C. L. Lin, and K. C. Fan, 2004, "Biometric verification using thermal images of palm-dorsa vein patterns," *IEEE Transactions on Circuits and Systems for Video Technology*, vol. 14, pp. 199–213.

N. Miura, A. Nagasaka, and T. Miyatake, 2004, "Feature extraction of finger vein patterns based on iterative line tracking and its application to personal identification," *Systems and Computers in Japan*, vol. 35, pp. 61–71.

R. P. Wildes, 1997, "Iris recognition: An emerging biometric technology," *in Proceedings of the IEEE*, vol. 85, pp. 1348–1363.

R. Hill, "Retina Identification", Chapter 4 in A., Jain, Bolle, and S., Pankanti, 1999, "*BIOMETRICS: Personal Identification in Networked Society*," 2nd Printing, Kluwer Academic Publishers.

R. Derakhshani, and A. Ross, 2006, "Conjunctival Scans for Personal Identification", provisional patent filed through UM system. File No. 05UMK074.

A. K. Jain, A. Ross, and S. Prabhakar, 2004, " An Introduction to Biometric Recognition", *IEEE Transactions on Circuits and Systems for Video Technology, Special Issue on Image- and Video-Based Biometrics*, vol. 14, No. 1, pp. 4-20.

C. Simon, and I. Goldstein, 1935, "A New Scientific Method of Identification," *New York State Journal of Medicine*, vol. 35, No. 18, pp. 901-906.

P. Tower, 1955, "The fundus Oculi in monozygotic twins: Report of six pairs of identical twins," *Archives of Ophthalmology*, vol. 54, pp. 225-239.

A. M. Joussen, 2001, "Vascular plasticity - the role of the angiopoietins in modulating ocular angiogenesis," *Graefe's Archive for Clinical and Experimental Ophthalmology*, vol. 239, Issue 12, pp. 972 - 975

C. G. Owen, T. J. Ellis, A. R. Rudnicka, and E.G. Woodward, 2002, "Optimal green (red-free) digital imaging of conjunctival vasculature." *Ophthalmic Physiol* Opt. vol. 22(3), pp. 234-43.

Q., Li, S., Sone, and K., Doi, 2003, "Selective enhancement filters for nodules, vessels, and airway walls in two-and three dimentional CT scans," *Medical Physics*, vol. 30, no. 8.

E. Martinez Perez, A. D. Hughes, A. V. Stanton, S. A. Tom, A. A. Bharath, and K. H. Parker, 1999, "Segmentation of retinal blood vessels based on the second directional derivative and region growing," *International Conference on Image Processing (ICIP)*, vol. 2, pp. 173–176.

M. K. Hu, 1962, "Visual Pattern Recognition by Moment Invariants", *IRE Trans. Info. Theory*, vol. IT-8, pp.179-187.